



Universiteit
Leiden
The Netherlands

Subarachnoid CSF hyperintensities at 7 tesla FLAIR MRI: a novel marker in cerebral amyloid angiopathy

Koemans, E.A.; Walderveen, M.A.A. van; Voigt, S.; Rasing, I.; Harten, T.W. van; Os, H.J.A. van; ... ; Wermer, M.J.H.

Citation

Koemans, E. A., Walderveen, M. A. A. van, Voigt, S., Rasing, I., Harten, T. W. van, Os, H. J. A. van, ... Wermer, M. J. H. (2023). Subarachnoid CSF hyperintensities at 7 tesla FLAIR MRI: a novel marker in cerebral amyloid angiopathy. *Neuroimage: Clinical*, 38. doi:10.1016/j.nicl.2023.103386

Version: Publisher's Version

License: [Creative Commons CC BY 4.0 license](https://creativecommons.org/licenses/by/4.0/)

Downloaded from: <https://hdl.handle.net/1887/3731219>

Note: To cite this publication please use the final published version (if applicable).



Subarachnoid CSF hyperintensities at 7 tesla FLAIR MRI: A novel marker in cerebral amyloid angiopathy

Emma A. Koemans^{a,*}, Marianne A.A. van Walderveen^b, Sabine Voigt^{a,b}, Ingeborg Rasing^a, Thijs W. van Harten^b, Hine J.A van Os^{a,c}, Nelleke van der Weerd^a, Gisela M. Terwindt^a, Matthias J.P. van Osch^b, Susanne J. van Veluw^{b,d,e}, Whitney M. Freeze^{b,1}, Marieke J. H. Wermer^{a,1}

^a Leiden University Medical Center, Department of Neurology, Leiden, The Netherlands

^b Leiden University Medical Center, Department of Radiology, Leiden, The Netherlands

^c Leiden University Medical Center, Department of Public Health, Leiden, The Netherlands

^d Massachusetts General Hospital, Harvard Medical School, J. Philip Kistler Stroke Research Center, Boston, MA, USA

^e Massachusetts General Hospital, MassGeneral Institute for Neurodegenerative Disease, Charlestown, MA, USA

ARTICLE INFO

Keywords:

Cerebral amyloid angiopathy
7 Tesla MRI
Cerebrospinal fluid hyperintensities
Cortical superficial siderosis

ABSTRACT

Background: We observed subarachnoid cerebrospinal fluid (CSF) hyperintensities at non-contrast 7-tesla (T) fluid-attenuated inversion recovery (FLAIR) MRI, frequently topographically associated with cortical superficial siderosis (cSS), in participants with cerebral amyloid angiopathy (CAA). To systemically evaluate these CSF hyperintensities we investigated their frequency and anatomical and temporal relationship with cSS on 7T and 3T MRI in hereditary Dutch-type CAA (D-CAA), sporadic CAA (sCAA), and non-CAA controls.

Methods: CAA participants were included from two prospective natural history studies and non-CAA controls from a 7T study in healthy females and females with ischemic stroke. CSF hyperintensities were scored by two independent observers.

Results: We included 38 sCAA participants (mean age 72y), 50 D-CAA participants (mean age 50y) and 44 non-CAA controls (mean age 53y, 15 with stroke). In total 27/38 (71 %, 95 %CI 56–84) sCAA and 23/50 (46 %, 95 %CI 33–60) D-CAA participants had subarachnoid CSF hyperintensities at baseline 7T. Most (96 %) of those had cSS, in 54 % there was complete topographical overlap with cSS. The remaining 46 % had ≥ 1 sulcus with CSF hyperintensities without co-localizing cSS. None of the healthy controls and 2/15 (13 %, 95 %CI 2–41, 100 % cSS overlap) of the stroke controls had CSF hyperintensities. In 85 % of the CAA participants CSF hyperintensities could retrospectively be identified at 3T. Of the 35 CAA participants with follow-up 7T after two years, 17/35 (49 %) showed increase and 6/35 (17 %) decrease of regional CSF hyperintensities. In 2/11 (18 %) of participants with follow-up who had baseline CSF hyperintensities without overlapping cSS, new cSS developed at those locations.

Conclusions: Subarachnoid CSF hyperintensities at 7T FLAIR MRI occur frequently in CAA and are associated with cSS, although without complete overlap. We hypothesize that the phenomenon could be a sign of subtle plasma protein or blood product leakage into the CSF, resulting in CSF T1-shortening.

Abbreviations: 95%CI, 95% confidence interval; 7T, 7 Tesla; 3T, 3 Tesla; CAA, Cerebral amyloid angiopathy; cSAH, Convexity subarachnoid hemorrhage; CSF, Cerebrospinal fluid; CSO-EPVS, Enlarged perivascular spaces in the centrum semiovale; cSS, Cortical superficial siderosis; cSVD, Cerebral small vessel disease; D-CAA, Hereditary Dutch-type CAA; FLAIR, Fluid-attenuated inversion recovery; FOV, Field-of-view; ICH, Intracerebral hemorrhage; LUMC, Leiden University Medical Center; sCAA, Sporadic CAA; STRIVE, Standards for Reporting Vascular changes on nEuroimaging; TR, Repetition time; TE, Echo time; TI, Inversion Time; WMH, White matter hyperintensities.

* Corresponding author at: Leiden University Medical Center, Albinusdreef 2, 2300 RC Leiden, The Netherlands.

E-mail address: e.a.koemans@lumc.nl (E.A. Koemans).

¹ Shared last authorship.

<https://doi.org/10.1016/j.nicl.2023.103386>

Received 27 December 2022; Received in revised form 25 February 2023; Accepted 24 March 2023

Available online 25 March 2023

2213-1582/© 2023 The Authors. Published by Elsevier Inc. This is an open access article under the CC BY license (<http://creativecommons.org/licenses/by/4.0/>).

1. Introduction

Hyperintensities of the subarachnoid cerebrospinal fluid (CSF) can be observed at Fluid Attenuated Inversion Recovery (FLAIR) MRI, as a result of an incomplete suppression of CSF signal due to T1 shortening. The phenomenon can be a sign of pathologies of the subarachnoid space and/or vessel wall permeability. (Althaus et al., 2022; Stuckey et al., 2007) In cerebral amyloid angiopathy (CAA), subarachnoid CSF hyperintensities on non-contrast 1.5T (T) or 3T FLAIR MRI are often considered a sign of acute convexity subarachnoid hemorrhage (cSAH): acute bleeding from the leptomeningeal vessels into the subarachnoid space. (Calviere et al., 2016) It is hypothesized that (repeated episodes of) cSAH can lead to cortical superficial siderosis (cSS), a hallmark hemorrhagic neuroimaging marker of CAA and one of the strongest predictors for intracerebral hemorrhage (ICH). (Charidimou et al., 2019; Charidimou et al., 2020; Linn et al., 2008) Other theories regarding cSS pathophysiology are that it is caused by more subtle, chronic leakage of blood and blood products from damaged leptomeningeal vessels into the subarachnoid space. (Charidimou et al., 2020).

We recently observed subarachnoid CSF hyperintensities on non-contrast 7T FLAIR MRI in research participants with sporadic CAA (sCAA) and hereditary Dutch-type CAA (D-CAA), who did not have symptoms of cSAH nor clear signs of cSAH at lower field (3T) FLAIR MRI. The subarachnoid CSF hyperintensities at 7T FLAIR MRI seemed to frequently overlap spatially with cSS on corresponding 7T T2*-weighted GRE scans. We hypothesized that the subarachnoid CSF hyperintensities seen at 7T MRI may be a sign of more subtle leptomeningeal vessel leakage of plasma proteins and/or erythrocytes, and therefore a possibly early sign of developing cSS. We aimed to explore the frequency, topographical association with cSS and temporal dynamics of this novel neuroimaging phenomenon at 7T FLAIR MRI in two prospective cohorts of participants with sCAA and D-CAA, and one with non-CAA controls. Furthermore, in retrospect we investigated the appearance of areas with 7T CSF hyperintensities on corresponding locations on 3T MRI. Lastly, to investigate our hypothesis that the hyperintensities are a sign of leptomeningeal vessel leakage, we investigated the relation between subarachnoid CSF hyperintensities and total protein levels in the CSF.

2. Materials and methods

2.1. Study participants

Participants with CAA were included from two prospective longitudinal natural history studies at the Leiden University Medical Center (LUMC): the FOCAS study, which includes participants with sporadic CAA (sCAA), and the AURORA study, which includes both symptomatic and pre-symptomatic participants with hereditary Dutch-type CAA (D-CAA). D-CAA is an autosomal dominant hereditary disease which is pathologically and radiologically similar to sCAA, although it has an earlier onset and more severe disease course. In contrast to sCAA, D-CAA can be diagnosed with certainty during life and is, therefore, often used as a genetic model for the disease. (van Etten et al., 2016) Participants were recruited via the (outpatient) clinic of the LUMC. For sCAA, the inclusion criteria were: (1). age ≥ 55 years, (2). probable CAA based on the modified Boston criteria diagnosed at 1.5T or 3T MRI, (3). ability and willingness to provide written informed consent. For D-CAA the inclusion criteria were: (1). age ≥ 18 years, (2). presence of the causal APP mutation OR a history of symptomatic ICH on CT/MRI suspect for CAA and at least 1 first-degree relative with D-CAA. In this study we consider participants with D-CAA to be symptomatic if they have suffered from at least one symptomatic ICH. To investigate whether the subarachnoid CSF hyperintensities at 7T FLAIR MRI were specific for CAA, and to evaluate the possibility of the finding being a 7T MRI-related artefact, we included a control group with ischemic stroke and a healthy control group without stroke from an 7T study in the LUMC (WHISPER study). Inclusion criteria for the WHISPER study were: (1).

female sex, (2). age between 40 and 60 years, (3). a history of ischemic stroke (only for the ischemic stroke group) and absence of any other neurological disorders, OR no history of any neurological disorder (including ischemic stroke) (for the healthy control group), (4). Absence of the following disorders: migraine, pre-eclampsia, systemic diseases associated with demyelinating or inflammatory white matter brain lesions. Participants were recruited via the (outpatient) clinic of the LUMC and via advertising. For this study, participants who were not able to undergo 7T MRI, or whose 7T FLAIR MRI could not be analyzed because of motion artifacts, were excluded.

2.1.1. Standard protocol Approvals, Registrations, and patient consents

The FOCAS, AURORA, and WHISPER studies were approved by the local ethics review board of the LUMC, and informed written consent was obtained from all participants.

2.2. Mri

2.2.1. Image acquisition

All participants underwent baseline MRI scanning on a whole body human 7T MR system (Philips, Best, the Netherlands) and part of the participants of the FOCAS and AURORA studies underwent a follow-up 7T MRI after two years. A quadrature transmit and 32-channel receive head coil (Nova Medical, Wilmington, MA, USA) was used and all participants were scanned according to a protocol which has been published in previous studies. (Koemans et al., 2021) The 7T scan protocol contained FLAIR images with the following parameters: repetition time (TR)/echo time (TE): 8000/328 ms, inversion time (TI): 2200 ms, 225 slices with no interslice gap, field-of-view (FOV) $250 \times 240 \times 180$ with a voxel size of $0.8 \times 0.8 \times 0.8$ mm (scan duration 12:08 min), and 2D flow-compensated transverse T2*-weighted GRE scanned with the following parameters: TR/TE 1851/25 ms, flip angle 60 degrees, slice thickness 1.0 mm with a 0.1 mm interslice gap, 92 slices (multiband factor 2) and coverage of 10 cm, $240 \times 180 \times 100$ mm FOV, 1000×751 matrix size – resulting in an in-plane spatial resolution of 0.24×0.24 mm (scan duration 10 min).

For participants of the FOCAS and AURORA study a 3T MRI scan of the brain was made on the same day as the baseline 7T scan. The 3T MRI (Philips, Best, the Netherlands) was performed using a standard 32-channel head coil (Philips, Best, the Netherlands), according to a previously published protocol. (Koemans et al., 2022) The scan protocol contained 3-dimensional FLAIR images with the following parameters: TR/TE = 4800/280 ms, inversion time (TI) 1650 ms, 321 slices with no interslice gap and an FOV of $250 \times 250 \times 180$ mm with a voxel size of $1.1 \times 1.1 \times 0.6$ mm (scan duration 4:43 min) and SWI with the following parameters: TR/TE = 31/7.2 ms, flip angle 17 degrees, 130 slices and an FOV of $230 \times 190 \times 130$ mm with a voxel size of $0.6 \times 0.6 \times 1$ mm (scan duration of 3:31 min).

2.2.2. Image analysis

In all participants, presence and location of subarachnoid CSF hyperintensities and cSS were scored on baseline and follow-up 7T FLAIR and T2*-weighted GRE images respectively. The presence of subarachnoid CSF hyperintensities and cSS at baseline was scored by two independent observers (E.A.K, >5 years of experience in the field, and W.M.F, >8 years of experience in the field), and discrepancies were evaluated during a consensus meeting. In case of uncertainty an experienced neuroradiologist (M.A.A.v.W., >15 years of experience in the field) was consulted. Subarachnoid CSF hyperintensities were defined as increased signal intensity in the subarachnoid space (in cortical sulci and/or on the surface of the cortex) on 7T FLAIR MRI with normal CSF hypointensity in the remaining subarachnoid and ventricular spaces (see Fig. 1).

We first analyzed the subarachnoid spaces on transverse 7T FLAIR MRI and confirmed our findings on sagittal and coronal reformatted images. We were careful to differentiate subarachnoid CSF

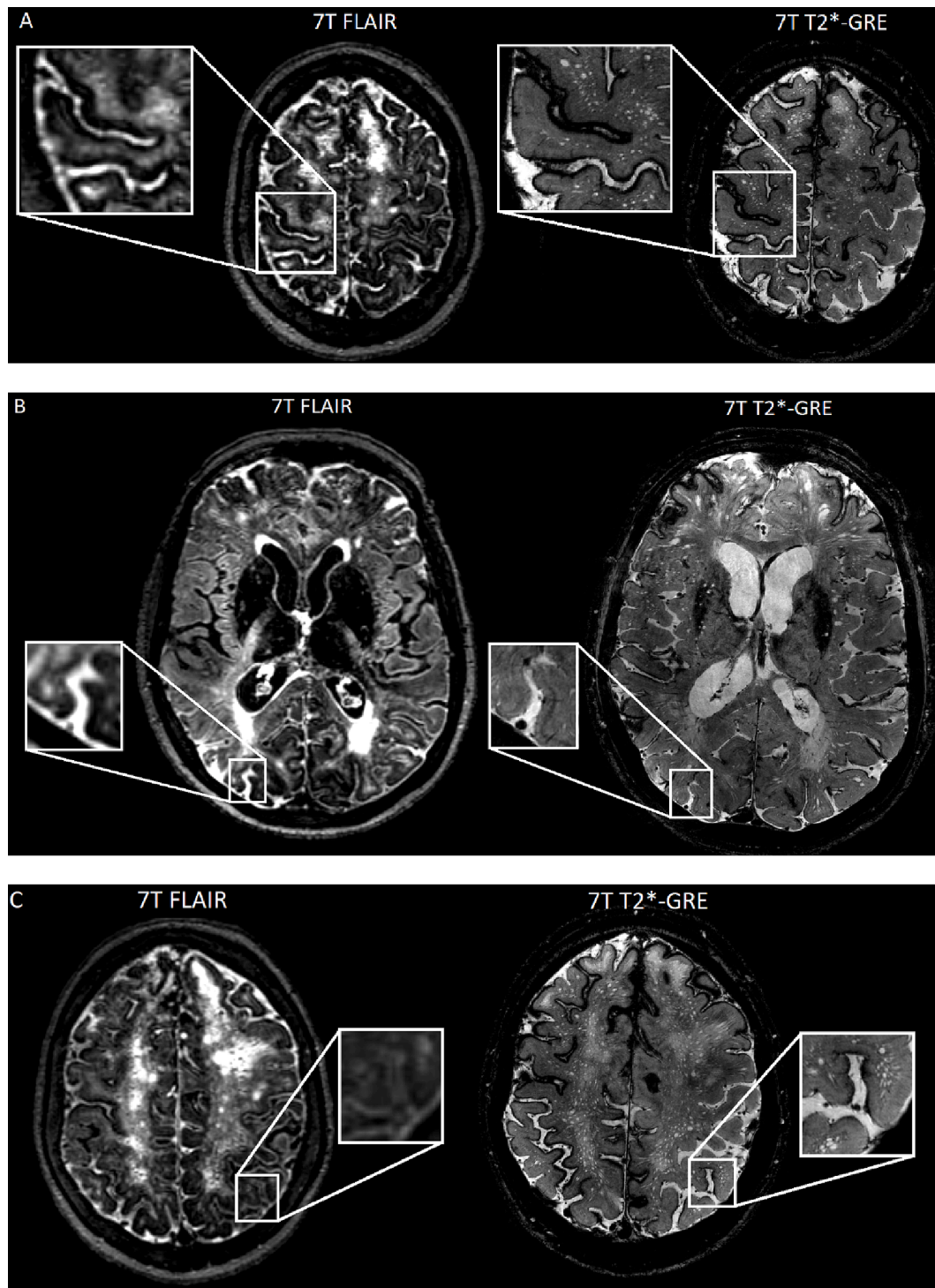


Fig. 1. CSF hyperintensities at 7T FLAIR in relation to cSS at 7T T₂*-GRE. CSF hyperintensities at 7T FLAIR and cSS at T₂*-GRE in a participant with sCAA; (A) example of multiple sulci with CSF hyperintensities at 7T FLAIR with complete overlapping cSS. (B) Example of a sulcus with CSF hyperintensities without overlapping cSS. (C) Example of a sulcus with cSS without overlapping CSF hyperintensities.

hyperintensities from the so called ‘hyperintense cortical rim’, a normal finding at 7T FLAIR MRI, also seen in healthy controls, which results from the amplification of the signal from superficial cortical layers at high field strength. (van Veluw et al., 2015) CSF hyperintensities in the subarachnoid spaces at the base of the temporal and frontal lobes as were observed in healthy controls (see Fig. 1 of the supplemental methods) and described in literature were discarded, because local incomplete nulling of CSF in these locations can be caused by air in the

paranasal sinuses and temporal bones and are therefore considered an MRI artefact. (Stuckey et al., 2007) We experienced difficulties with distinguishing CSF hyperintensities in the temporal lobe from artefacts (see supplemental Fig. 1), and therefore decided to separately report cases with CSF hyperintensities exclusively located within the temporal lobe. cSS was defined as homogeneous hypointense curvilinear signal loss outlining the surface of the cerebral cortex on T₂*-weighted GRE images. (Charidimou et al., 2015) A single rater (E.A.K) visually assessed

presence of subarachnoid CSF hyperintensities and cSS separately for each lobe (frontal, parietal, occipital, temporal). For each participant, focality score for the severity of subarachnoid CSF hyperintensities and cSS was determined for each case based on previously published scores created for cSS: a focal pattern indicated involvement of ≤ 3 sulci, a disseminated pattern indicated involvement of >3 sulci. (Linn et al., 2010) Spatial overlap of subarachnoid CSF hyperintensities and cSS was scored by detailed inspection of the 7T FLAIR and T2*-weighted GRE images, side-by-side, in the transversal plane. The presence and location of subarachnoid spaces with either CSF hyperintensities but no cSS, and/or cSS but no CSF hyperintensities, were documented. Regarding the foci with subarachnoid CSF hyperintensities, participants were categorized as follows: 1.) None of subarachnoid spaces with CSF hyperintensities have overlapping cSS, 2.) ≤ 50 % of subarachnoid spaces with CSF hyperintensities have overlapping cSS, 3.) >50 % of subarachnoid spaces with CSF hyperintensities have overlapping cSS, 4.) All subarachnoid spaces with CSF hyperintensities have overlapping cSS. Furthermore, the presence, location, and overlap of subarachnoid CSF hyperintensities and cSS on follow-up 7T FLAIR MRI scans was compared side-by-side with the baseline scans by a single rater (E.A.K.). Lastly, for all participants of the AURORA and FOCAS studies with subarachnoid CSF hyperintensities at 7T FLAIR, baseline 3T FLAIR images were inspected to see if any (subtle) signal attenuation in the corresponding subarachnoid spaces could be identified in retrospect.

The following cerebral small vessel disease (cSVD) MRI markers were scored, according to the Standards for Reporting Vascular changes on nEuroimaging (STRIVE) criteria, in the participants with CAA at baseline 3T MRI by a single observer (E.A.K.): microbleeds, macrobleeds, cSS, cSAH, white matter hyperintensities (WMH) and enlarged perivascular spaces in the centrum semiovale (CSO-EPVS).

2.3. Lumbar puncture and CSF analyses

As we hypothesized that the subarachnoid CSF hyperintensities might be a sign of leptomeningeal vessels leaking plasma proteins, we investigated differences in CSF protein levels between participants with and without CSF hyperintensities at 7T FLAIR: a subset of participants with CAA consented to lumbar punctures for CSF analysis as part of the FOCAS and AURORA research protocols. Lumbar punctures were performed on the same day as the 7T MRI, under standardized conditions. Samples were collected in polypropylene tubes and transferred to the clinical laboratory of the LUMC within 30 min, where routine CSF analyses for total protein levels were performed.

2.4. Statistics

Descriptive statistics were used to calculate frequencies, means and medians of baseline characteristics for all four participant groups (D-CAA, sCAA, controls with a history of stroke, healthy controls). The frequency of the occurrence of subarachnoid CSF hyperintensities at 7T FLAIR MRI was calculated including 95 % confidence intervals (95 % CI) for each group separately. Inter-rater reliability for determining the presence of CSF hyperintensities and cSS was computed with Cohen's κ . The association between the presence of CSF hyperintensities and cSS was assessed with the Chi-squared test. The association between the presence of CSF hyperintensities and total CSF protein levels in participants with CAA was assessed with multiple linear regression, corrected for age at baseline, sex, and type of CAA (sCAA or D-CAA). An $\alpha < 0.05$ was applied to determine statistical significance and all p-values are two-tailed.

2.5. Data availability

Further information about the dataset can be obtained from the corresponding author upon reasonable request.

3. Results

In total, 132 participants were included at baseline: 38 participants with sCAA (mean age 72 years, 40 % female), 50 participants with D-CAA (mean age 50 years, 56 % female, 48 % symptomatic) and 44 non-CAA controls (mean age 53 years, 100 % female, 15 with a history of ischemic stroke and 29 without). See Fig. 2 in the supplemental methods for the flowchart detailing inclusion of the participants. For baseline characteristics see Table 1.

3.1. Frequency of subarachnoid CSF hyperintensities

Subarachnoid CSF hyperintensities at baseline 7T FLAIR MRI were observed in 27/38 (71 %, 95 % CI 56–84) of the participants with sCAA (19/25 (76 %) with and eight/13 (62 %) without a previous symptomatic ICH) and 23/50 (46 %, 95 % CI 33–60) of the participants with D-CAA (20/24 (83 %) of participants with previous ICH and three/26 (12 %) of pre-symptomatic participants). In 44/50 (88 %) participants with CAA the subarachnoid CSF hyperintensities showed a disseminated pattern, and the hyperintensities occurred most often in the parietal and frontal lobes (Table 2). Of the non-CAA control participants, two/15 (13 %, 95 % CI 2–41) of the participants with a history of ischemic stroke and 0/29 (0 %, 95 % CI 0–12) healthy controls had focal subarachnoid CSF hyperintensities at 7T FLAIR MRI (Table 2). Inter-rater reliabilities for the assessment of presence of subarachnoid CSF hyperintensities (Cohen's κ [95 % CI] = 0.905 [0.832; 0.979]) and cSS (Cohen's κ [95 % CI] = 0.921 [0.853; 0.989]) were excellent.

3.2. Co-localization of subarachnoid CSF hyperintensities with cSS

There was a strong association between the presence of CSF hyperintensities and cSS ($\chi^2 = 62.66$, $p < 0.001$). In sCAA and D-CAA, 48/50 (96 %) of participants with subarachnoid CSF hyperintensities had cSS. The three presymptomatic participants with D-CAA with CSF hyperintensities all also had cSS on MRI. Most but not all CSF hyperintensities were associated locally with cSS on the corresponding T2*-GRE: in 27/50 (54 %) of participants all subarachnoid CSF hyperintensities had complete overlapping cSS. In 17/50 (34 %) participants > 50 % of CSF hyperintensities had overlapping cSS, in four/50 (8 %) of participants ≤ 50 % of CSF hyperintensities had overlapping cSS, and in two/50 (4 %) of participants none of the subarachnoid CSF hyperintensities had overlapping cSS (see Table 2; Fig. 1). The two non-CAA control participants with subarachnoid CSF hyperintensities at 7T FLAIR MRI both had complete overlapping cSS. One of them showed signs of a lobar ICH or hemorrhagic transformation in an ischemic infarct (a clear distinction could not be made) close to the location of the cSS. The other participant did not have any other cSVD MRI markers. There were no other non-CAA control participants with cSS.

Finally, not all participants with cSS had complete overlapping subarachnoid CSF hyperintensities: 37/52 (71 %) of CAA participants with cSS had at least one sulcus of cSS which did not overlap with CSF hyperintensities (see Fig. 1).

3.3. Temporal dynamics of CSF hyperintensities

In ten participants with sCAA and 25 participants with D-CAA a follow-up 7T MRI was performed after two years. In total 17/35 (49 %) participants with follow-up 7T had new foci or extension of previous foci of CSF hyperintensities at 7T MRI; three of those 17 did not have CSF hyperintensities at baseline 7T. In nine/17 participants with new CSF hyperintensities at follow-up there was complete overlap of the new foci with cSS (six of those nine participants already had cSS present at baseline within some of the subarachnoid spaces with new CSF hyperintensities) (see Fig. 2A). The other eight/17 participants with new CSF hyperintensities at follow-up had at least one focus with new CSF hyperintensities that did not overlap with cSS at follow-up. In six/35

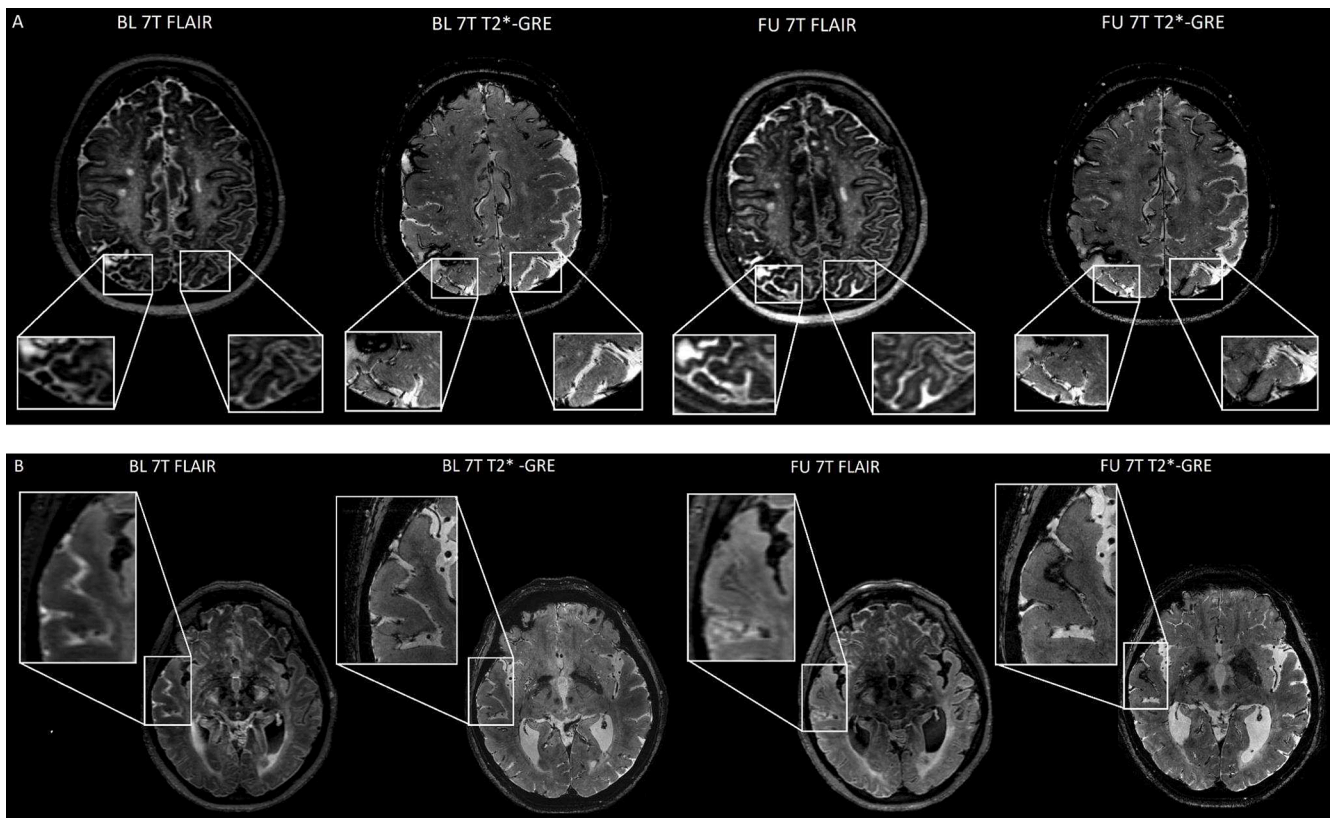


Fig. 2. Examples of dynamic temporal evolution of CSF hyperintensities in CAA. Follow up of CSF hyperintensities in a participant with D-CAA, 2A: progression of subtle CSF hyperintensities with subtle cSS to more prominent CSF hyperintensities in a right parietal sulcus (left box), and new CSF hyperintensities with new cSS in a left parietal sulcus (right box). 2B: New cSS at region with CSF hyperintensities without cSS at baseline.

participants with follow-up 7T CSF hyperintensities disappeared in at least one focus (see Fig. 2). Of the 23 participants who had baseline CSF hyperintensities without cSS, eleven had a follow-up 7T-MRI after 2 years. Two of those had new cSS at those locations (Fig. 2B).

3.4. Subarachnoid CSF hyperintensities, cSS and cSAH on 3T MRI

Of the CAA participants with CSF hyperintensities, 19 participants with sCAA and 14 participants with D-CAA had a 3T MRI FLAIR performed on the same day as the 7T MRI. Upon initial, blinded assessment of the 3T FLAIR MRI scans, none of the scans was considered to be positive for signs of subarachnoid hyperintensities corresponding to cSAH at 3T FLAIR. However, after side-by-side comparison of the 3T FLAIR with the 7T FLAIR scans, in 28/33 (85 %) participants some incomplete subarachnoid signal attenuation corresponding locally to the subarachnoid CSF hyperintensities seen at 7T could be seen in retrospect. The poorer signal attenuation within subarachnoid spaces with CSF hyperintensities at 7T FLAIR MRI was generally less conspicuous at 3T FLAIR MRI, and the signal intensity within the sulci was non-uniform (Fig. 3).

3.5. CSF hyperintensities and total protein levels in CSF

Total protein levels in the CSF were assessed in 13 participants with D-CAA (mean (sd) = 0.40 (0.10)), 3/13 with subarachnoid CSF hyperintensities at baseline 7T FLAIR and 7 participants with sCAA (mean (sd) = 0.35 (0.09)), 6/7 with subarachnoid CSF hyperintensities at baseline 7T FLAIR. CSF total protein levels were not associated with the presence of CSF hyperintensities in the sCAA and D-CAA participant groups combined after correcting for age, sex, and CAA type ($B = -0.001$, $t = -0.22$, $p = 0.983$, see supplemental Fig. 3).

4. Discussion

In this study we found that CSF hyperintensities at 7T FLAIR are a frequent finding in both sCAA and D-CAA, frequently (but not always) overlapping with cSS. Incomplete attenuation of the CSF signal was apparent at 3T MRI in retrospect, albeit more subtly, in most participants. The subarachnoid CSF hyperintensities at 7T FLAIR varied over a timeframe of two years: in approximately half of the participants with a follow-up MRI scan new sulci with CSF hyperintensities appeared, and in 17 % of participants foci with CSF hyperintensities that were visible at baseline could no longer be seen at follow-up.

The mechanisms underlying the neuroradiological phenomenon described here and the reason for its relatively strong association with cSS are yet uncertain. It can be hypothesized that the subarachnoid 7T FLAIR hyperintensities are caused by local chronic, subtle leakage of plasma proteins or blood products from fragile CAA-affected leptomeningeal vessels, possibly eventually resulting cSS in some cases. The high rate of co-localization between the two markers suggests that this could be true, however the follow-up data supports this only in a minority of participants. FLAIR hyperintensities are characteristic for diseases with pathology located within or adjacent to the CSF subarachnoid space, such as SAH, meningitis, or leptomeningeal metastasis. (Stuckey et al., 2007) It is also well-known that CSF hyperintensities can occur on post-contrast FLAIR images due to blood-brain barrier (BBB) leakage of gadolinium-based contrast material. (Freeze et al., 2020) In all of these conditions, the CSF signal is no longer fully suppressed by the inversion pulse due to shortening of the T1-relaxation time of CSF, for example caused by increased protein levels, blood products, or contrast material. (Stuckey et al., 2007) In this study, no relation was found between CSF hyperintensities at 7T and CSF protein levels, although this analysis might be underpowered due to the small sample size of participants who underwent lumbar puncture. In accordance with our

Table 1
Baseline characteristics.

	sCAA (n = 38)	D-CAA (n = 50)	Stroke controls (n = 15)	Healthy controls (n = 29)
Mean age at baseline 7T MRI (range)	72 (62–86)	50 (26–75)	53 (45–60)	53 (43–59)
Females (%)	15 (40)	28 (56)	15 (100)	29 (100)
Symptomatic ICH [‡] (%)	25 (66)	24 (48)	0 (0)	0 (0)
<i>Characteristics at 3T MRI</i>				
Median microbleed number (range)	57 (0–1244) [‡]	70 (0–1906)	–	–
Median macrobleed number (range)	5 (0–55) [†]	6 (0–86)	–	–
Mixed-type cSVD (%)	9 (24)	0 (0)	–	–
cSS (%) [†]	21 (55)	16 (32)	–	–
Subarachnoid hemorrhage (%)	0 (0)	0 (0)	–	–
Median periventricular WMH FAZEKAS score (range)	3 (0–3)	2 (0–3)	–	–
Median deep WMH FAZEKAS score (range)	2 (0–3)	2 (0–3)	–	–
Median CSO-EPVS score (range)	4 (2–4)	4 (1–4) [§]	–	–

sCAA = sporadic CAA; D-CAA = hereditary Dutch type CAA; ICH = intracerebral hemorrhage; cSVD = cerebral small vessel disease; cSS = cortical superficial siderosis; WMH = white matter hyperintensities; CSO-EPVS = enlarged perivascular spaces in the centrum semiovale.

* Diagnosis of sICH made based on clinical signs and symptoms primarily, and evidence of hemorrhage on imaging secondary.

[†] cSS < 3 sulci from ICH is not included.

[‡] Data from one case with sCAA are missing; [§]Data from one case with D-CAA are missing.

findings, a previous study that assessed cSS in a memory clinic population found no association between cSS and the CSF/serum albumin ratio. (Shams et al., 2016) In our current study the CSF hyperintensities were not only found in participants with CAA, but also in two non-CAA control participants with ischemic stroke. The marker might therefore not be unique to CAA. Of note, both control participants had cSS in the same area, but did not have any other MRI markers suggestive for CAA. Although cSS is strongly related to CAA, it can also be caused by red blood cell extravasation from other causes such as aneurysmatic vessel rupture or trauma; in these control participants the cause of the cSS is unknown. (Shams et al., 2016; Iannaccone et al., 1999) CSF hyperintensities were found in all regions of the brain, but most frequently in the frontal and parietal lobe, which corresponds to the locations where cSS is predominantly observed. (Linn et al., 2010; Zonneveld et al., 2014) The two control subjects with CSF hyperintensities both had a history of ischemic stroke; none of the healthy control subjects had any evidence of CSF hyperintensities. If, hypothetically, CSF hyperintensities were to reflect vessel leakage, this phenomenon might not only be present in CAA but also in other cSVDs with damage to the leptomeningeal vasculature. (Freeze et al., 2019) Our study would then demonstrate that widespread (subtle) vessel leakage is present even in early stages of (D-)CAA, which would aid the understanding of CAA pathophysiology in general and (considering the possible overlap with) cSS in particular. Hypothetically, this could have future implications for management as vessel leakage could be a target for therapy, and cSS is an important prognostic marker for future ICH. However, more studies, preferably using contrast-enhanced MRI, are definitely needed to further investigate whether CSF hyperintensities indeed reflect vessel leakage and are associated with cSS.

An alternative explanation for the CSF hyperintensities could be that subarachnoid CSF hyperintensities are caused by magnetic field inhomogeneities induced by iron molecules that are present within areas

Table 2
Characteristics of subarachnoid CSF hyperintensities at 7T FLAIR MRI.

	sCAA (n = 38)	D-CAA (n = 50)	Stroke controls (n = 15)	Healthy controls (n = 29)
CSF hyperintensities at baseline 7T FLAIR(%)	27 (71)	23 (46)	2 (13)	0
Frontal (%)	22 (81)	20 (87)	2 (100)	0
Parietal (%)	25 (93)	22 (96)	1 (50)	0
Temporal (%)	16 (59)	6 (26)	0	0
Occipital (%)	20 (74)	18 (78)	0	0
Focal (%)	4 (11)	2 (9)	1 (50)	0
Disseminated (%)	23 (85)	21 (91)	1 (50)	0
CSF hyperintensities without cSS (%)	11 (41)	12 (52)	0	0
0 % of CSF hyperintensities have overlapping cSS (%)	2 (18)	0 (0)	0	0
≤50 % of CSF hyperintensities have overlapping cSS (%)	1 (9)	3 (25)	0	0
>50 % of CSF hyperintensities have overlapping cSS (%)	8 (73)	9 (75)	0	0
cSS without CSF hyperintensities (%)	18 (67)	17 (74)	0	0
CSF hyperintensities at 3T MRI/Total available 3T MRI (%)	15/29 (52)	13/40 (33)	–	–
cSS at baseline 7T (%)	27 (71) ²	25 (50) ²	2 (13)	0
<i>Follow up 7T MRI</i>	sCAA (n = 10)	D-CAA (n = 25)	–	–
CSF hyperintensities at FU 7T (%)	8 (80)	13 (52)	–	–
Participants with new CSF hyperintensities compared to baseline (%)	7 (70)	10 (40)	–	–
Participants with disappearance of CSF hyperintensities compared to baseline (%)	3 (30)	3 (12)	–	–

sCAA = sporadic CAA; D-CAA = hereditary Dutch type CAA; 7T = 7T; cSS = cortical superficial siderosis. ²Including n = 3 participants with sCAA and n = 1 participant with D-CAA who did have cSS at 7T MRI but only <3 sulci of an ICH.

of cSS, which may result in incomplete nulling of CSF. (Tha et al., 2009) In the present study, the CSF hyperintensities were clearly visible at 7T FLAIR, but were only noticed in retrospect at 3T FLAIR. A reason for this might be that ultra-high field strength could be more sensitive for shortening of the T1-relaxation time in CSF, or to magnetic susceptibility effects due to its increased signal-to-noise ratio. This has been previously described in literature as a problem increasing with field-strength, causing incomplete CSF nulling in areas such as the ventricles. (Zwanenburg et al., 2010) However, in this study we also found locations of CSF hyperintensities without evidence of cSS, as well as areas with cSS which did not have CSF hyperintensities. Therefore, a magnetic field effect of cSS does not seem to fully explain the phenomenon. Another possible explanation could be that the hyperintensities are caused by changes in water exchange affecting the effective T1, although we are unsure how CAA pathology would influence this.

The subarachnoid CSF hyperintensities showed variability over time: 49 % of participants had an increase in the count of foci with CSF hyperintensities (in 6 cases in locations where cSS was already present at baseline) and 17 % had a decrease in the count of subarachnoid spaces with CSF hyperintensities at follow-up 7T. This might indicate that CSF hyperintensities are a possible dynamic marker of cSVD. If CSF hyperintensities reflect subtle vascular leakage they may possibly serve as a marker for widespread leptomeningeal vessel fragility or remodeling, which might predispose to the development of vessel rupture and ICH. (Charidimou et al., 2020; Freeze et al., 2019) As the marker was also present in 12 % of pre-symptomatic participants with D-CAA, it might be

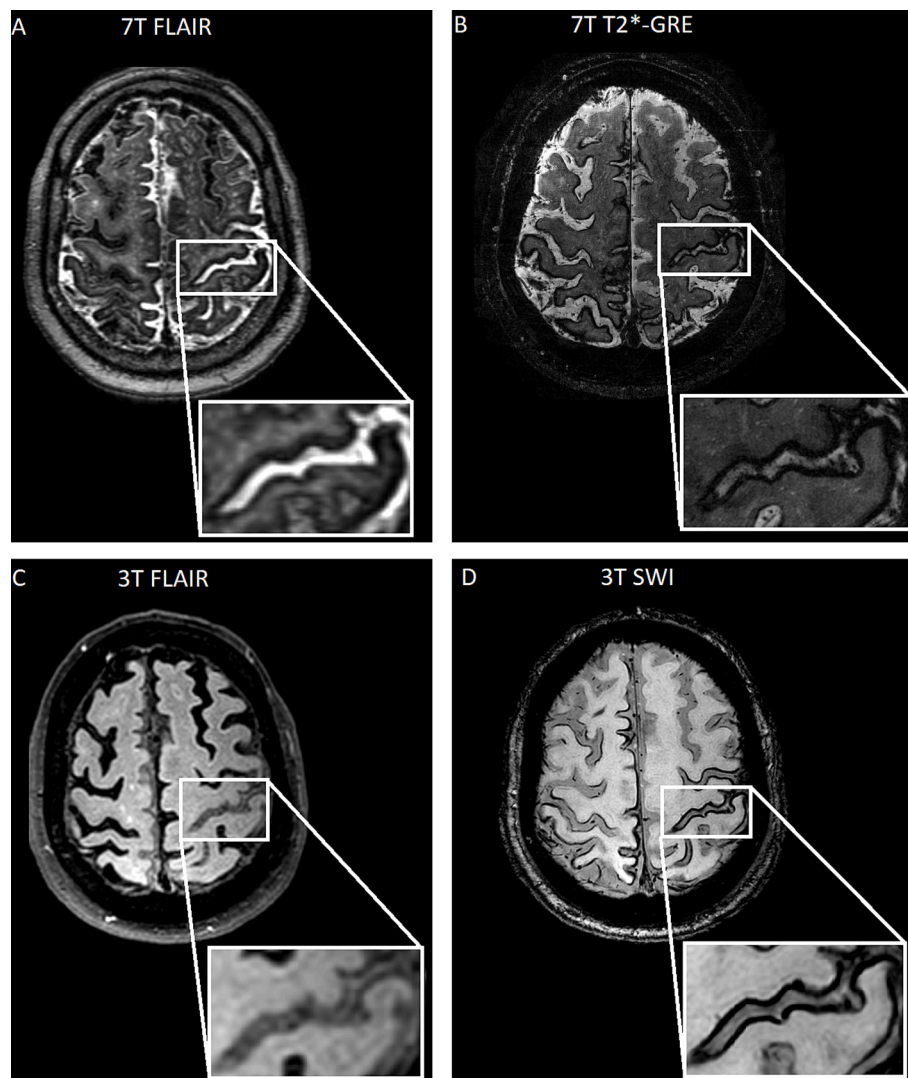


Fig. 3. CSF hyperintensities at 7T versus 3T MRI. Sulci with subarachnoid CSF hyperintensities and corresponding cSS (white box), and sulci with cSS without corresponding subarachnoid CSF hyperintensities (white arrow) at (3A) 7T FLAIR, (3B) 7T T₂*-GRE, (3C) 3T FLAIR, (3D) 3T SWI in the same participant with sCAA.

an early marker reflecting pre-symptomatic cSVD disease activity.

Some advantages of this study are the inclusion of both participants with sCAA and participants with hereditary D-CAA: inclusion of D-CAA allows for a diagnosis of definite CAA during life as well as investigation of the disease in individuals during their early pre-symptomatic phases. Another advantage is the use of both high-field 7T and 3T MRI performed on the same day, collected via a prospective study design at two time points: the high-field 7T allows for more detailed investigation of brain tissue and novel markers, whereas the comparison with 3T allows for a clearer translation to clinical practice.

Our study has several limitations. First, we were not able to validate the findings in this study via post-mortem neuropathological samples or investigate them in more detail via MRI scans with contrast, as these data are not available for the cohorts used in this study. The occurrence of FLAIR hyperintensities on contrast-enhanced MRI has been associated with renal insufficiency. Unfortunately we were not informed about the renal function of our participants, but none of them had a history of kidney disease. Second, we chose to visually assess the frequency, locations and overlap of subarachnoid CSF hyperintensities and cSS at 7T and 3T, and therefore there might have been an imperfect co-registration between FLAIR and GRE scans. However, we reformatted our 3D FLAIR sequence to match the GRE scans, enabling near perfect comparison. Furthermore, our methods are more similar to methods

used in everyday clinical practice, and the CSF hyperintensities were scored by two experienced, independent observers and discussed with an experienced clinical neuroradiologist. Third, the participants with sCAA are on average older than the control subjects, and age may be a factor contributing to the high frequency of CSF hyperintensities in this group. Lastly, lumbar punctures were performed in a relatively small sample size of participants, which made this particular sub-analysis likely to be underpowered. If local CSF hyperintensities influence local CSF protein levels, these differences may be very subtle and might not increase total protein levels as measured by lumbar puncture.

4.1. Conclusion

In this study subarachnoid CSF hyperintensities at 7T FLAIR MRI occurred frequently in participants with (pre-) symptomatic CAA, and were related to presence of cSS. Subarachnoid CSF hyperintensities showed variability over time and were found in some cases to herald future cSS. Further research in larger, longitudinal cohorts including MRI scans with contrast is necessary to determine the underlying pathophysiology and prognostic value of the marker, as well as to further investigate the hypothesis of subarachnoid CSF hyperintensities at 7T FLAIR MRI as an early sign of leptomeningeal vessel leakage and a possible precursor of cSS.

Funding sources

This work was supported by a Clinical Established Investigator grant of the Netherlands Heart Foundation 2016T086 to M.J.H. Wermer and by the Dutch CAA foundation. The funding agencies had no role in the design or conduct of the study.

Financial disclosure statement:

E.A. Koemans reports independent support in the form of travel grants from Alzheimer Nederland, the Dutch Heart foundation and KNAW van Leersum, and from the Dutch CAA foundation.

M.A.A. van Walderveen, S. Voigt, I. Rasing, T.W. van Harten, H.J.A. van Os and N. van der Weerd report no disclosures.

G.M. Terwindt reports independent support from de Nederlandse Organisatie voor Wetenschappelijk Onderzoek, European Community, the Dutch Heart Foundation, the Dutch Brain Foundation, and the Dutch CAA foundation.

M.J.P. van Osch reports support by a NWO-VICI grant (016.160.351) and a NWO- Human Measurement Models 2.0 grant (18969) as well as support from Nederlandse Organisatie voor Wetenschappelijk Onderzoek, European Community, the Dutch Heart Foundation, and the Dutch Brain Foundation.

S.J. van Veluw reports independent support from de Nederlandse Organisatie voor Wetenschappelijk Onderzoek ZonMw (VENI grant 91619021).

W.M. Freeze reports independent support from Alzheimer Nederland (WE.03-2018013) and the Alzheimer's Disease Research program of the BrightFocus Foundation (A2021007F).

M.J.H. Wermer reports independent support from de Nederlandse Organisatie voor Wetenschappelijk Onderzoek ZonMw (VIDI grant 91717337), the Netherlands Heart Foundation, and the Dutch CAA foundation.

CRedit authorship contribution statement

Emma A. Koemans: Conceptualization, Methodology, Validation, Formal analysis, Investigation, Writing – original draft, Resources. **Marianne A.A. van Walderveen:** Conceptualization, Methodology, Writing – review & editing, Supervision. **Sabine Voigt:** Resources, Conceptualization, Writing – review & editing. **Ingeborg Rasing:** Resources, Conceptualization, Writing – review & editing. **Thijs W. van Harten:** Resources, Writing – review & editing. **Hine J.A van Os:** Resources, Writing – review & editing. **Nelleke van der Weerd:** Resources, Writing – review & editing. **Gisela M. Terwindt:** Conceptualization, Writing – review & editing. **Matthias J.P. van Osch:** Conceptualization, Methodology, Supervision, Writing – review & editing. **Susanne J. van Veluw:** Conceptualization, Methodology, Supervision, Writing – review & editing. **Whitney M. Freeze:** Conceptualization, Methodology, Validation, Writing – original draft, Writing – review & editing, Supervision. **Marieke J.H. Wermer:** Conceptualization, Writing – review & editing, Supervision, Funding acquisition.

Declaration of Competing Interest

The authors declare that they have no known competing financial interests or personal relationships that could have appeared to influence the work reported in this paper.

Data availability

Data will be made available on request.

Appendix A. Supplementary data

Supplementary data to this article can be found online at <https://doi.org/10.1016/j.nicl.2023.103386>.

References

- Althaus, K., Kasel, M., Ludolph, A.C., Kassubek, J., Kassubek, R., 2022. HARM revisited: etiology of subarachnoid hyperintensities in brain FLAIR MRI. *Int. J. Stroke* 17 (10), 1121–1128.
- Calviere, L., Cuvinciu, V., Raposo, N., Faury, A., Cognard, C., Larrue, V., Viguier, A., Bonneville, F., 2016. Acute convexity subarachnoid hemorrhage related to cerebral amyloid angiopathy: Clinicoradiological features and outcome. *J. Stroke Cerebrovasc. Dis.* 25 (5), 1009–1016.
- Charidimou, A., Linn, J., Vernooij, M.W., Opherk, C., Akoudad, S., Baron, J.-C., Greenberg, S.M., Jäger, H.R., Werring, D.J., 2015. Cortical superficial siderosis: detection and clinical significance in cerebral amyloid angiopathy and related conditions. *Brain J. Neurol.* 138 (8), 2126–2139.
- Charidimou, A., Boulouis, G., Greenberg, S.M., Viswanathan, A., 2019. Cortical superficial siderosis and bleeding risk in cerebral amyloid angiopathy: A meta-analysis. *Neurology* 93 (24), e2192–e2202.
- Charidimou, A., Perosa, V., Frosch, M.P., Scherlek, A.A., Greenberg, S.M., van Veluw, S.J., 2020. Neuropathological correlates of cortical superficial siderosis in cerebral amyloid angiopathy. *Brain J. Neurol.* 143, 3343–3351.
- Freeze, W.M., Bacskai, B.J., Frosch, M.P., Jacobs, H.I.L., Backes, W.H., Greenberg, S.M., van Veluw, S.J., 2019. Blood-brain barrier leakage and microvascular lesions in cerebral amyloid angiopathy. *Stroke* 50 (2), 328–335.
- Freeze, W.M., van der Thiel, M., de Bresser, J., Klijn, C.J.M., van Etten, E.S., Jansen, J.F.A., et al., 2020. Csf enhancement on post-contrast fluid-attenuated inversion recovery images; a systematic review. *NeuroImage Clinical* 28, 102456.
- Iannaccone, S., Golzi, V., Sferrazza, B., Rino, F., Smirne, S., Ferini-Strambi, L., 1999. Central nervous system superficial siderosis, headache, and epilepsy. *Headache* 39 (9), 666–669.
- Koemans, E.A., Voigt, S., Rasing, I., Jolink, W.M.T., van Harten, T.W., van der Grond, J., van Rooden, S., Schreuder, F.H.B.M., Freeze, W.M., van Buchem, M.A., van Zwet, E.W., van Veluw, S.J., Terwindt, G.M., van Osch, M.J.P., Klijn, C.J.M., van Walderveen, M.A.A., Wermer, M.J.H., 2021. Striped occipital cortex and intragyrar hemorrhage: Novel magnetic resonance imaging markers for cerebral amyloid angiopathy. *Int. J. Stroke* 16 (9), 1031–1038.
- Koemans, E.A., Voigt, S., Rasing, I., van Harten, T.W., Jolink, W.M.T., Schreuder, F.H.B.M., van Zwet, E.W., van Buchem, M.A., van Osch, M.J.P., Terwindt, G.M., Klijn, C.J.M., van Walderveen, M.A.A., Wermer, M.J.H., 2022. Cerebellar superficial siderosis in cerebral amyloid angiopathy. *Stroke* 53 (2), 552–557.
- Linn, J., Herms, J., Dichgans, M., Brückmann, H., Fesl, G., Freilinger, T., Wiesmann, M., 2008. Subarachnoid hemosiderosis and superficial cortical hemosiderosis in cerebral amyloid angiopathy. *AJNR Am. J. Neuroradiol.* 29 (1), 184–186.
- Linn, J., Halpin, A., Demaerel, P., Ruhlmann, J., Giese, A.D., Dichgans, M., van Buchem, M.A., Bruckmann, H., Greenberg, S.M., 2010. Prevalence of superficial siderosis in patients with cerebral amyloid angiopathy. *Neurology* 74 (17), 1346–1350.
- Shams, S., Martola, J., Charidimou, A., Cavallini, L., Granberg, T., Shams, M., Forslin, Y., Aspelin, P., Kristoffersen-Wiberg, M., Wahlund, L.-O., 2016. Cortical superficial siderosis: Prevalence and biomarker profile in a memory clinic population. *Neurology* 87 (11), 1110–1117.
- Stuckey, S.L., Goh, T.D., Heffernan, T., Rowan, D., 2007. Hyperintensity in the subarachnoid space on flair mri. *AJF Am. J. Roentgenol.* 189 (4), 913–921.
- Tha, K.K., Terae, S., Kudo, K., Miyasaka, K., 2009. Differential diagnosis of hyperintense cerebrospinal fluid on fluid-attenuated inversion recovery images of the brain. Part ii: Non-pathological conditions. *Br. J. Radiol.* 82 (979), 610–614.
- van Etten, E.S., Gurol, M.E., van der Grond, J., Haan, J., Viswanathan, A., Schwab, K.M., Ayres, A.M., Algra, A., Rosand, J., van Buchem, M.A., Terwindt, G.M., Greenberg, S.M., Wermer, M.J.H., 2016. Recurrent hemorrhage risk and mortality in hereditary and sporadic cerebral amyloid angiopathy. *Neurology* 87 (14), 1482–1487.
- van Veluw, S.J., Fracasso, A., Visser, F., Spliet, W.G.M., Luijten, P.R., Biessels, G.J., Zwanenburg, J.J.M., 2015. Flair images at 7 tesla mri highlight the ependyma and the outer layers of the cerebral cortex. *Neuroimage* 104, 100–109.
- Zonneveld, H.I., Goos, J.D.C., Wattjes, M.P., Prins, N.D., Scheltens, P., van der Flier, W.M., Kuijer, J.P.A., Muller, M., Barkhof, F., 2014. Prevalence of cortical superficial siderosis in a memory clinic population. *Neurology* 82 (8), 698–704.
- Zwanenburg, J.J., Hendrikse, J., Visser, F., Takahara, T., Luijten, P.R., 2010. Fluid attenuated inversion recovery (flair) mri at 7.0 tesla: Comparison with 1.5 and 3.0 tesla. *Eur. Radiol.* 20, 915–922.